EXHIBIT J

Rapidly maturing variants of the *Discosoma* red fluorescent protein (DsRed)

Brooke J. Bevis and Benjamin S. Glick*

The red fluorescent protein DsRed has spectral properties that are ideal for dual-color experiments with green fluorescent protein (GFP)[1]. But wild-type DsRed has several drawbacks, including slow chromophore maturation and poor solubility[2,3]. To overcome the slow maturation, we used random and directed mutagenesis to create DsRed variants that mature 10–15 times faster than the wild-type protein. An asparagine-to-glutamine substitution at position 42 greatly accelerates the maturation of DsRed, but also increases the level of green emission. Additional amino acid substitutions suppress this green emission while further accelerating the maturation. To enhance the solubility of DsRed, we reduced the net charge near the N terminus of the protein. The optimized DsRed variants yield bright fluorescence even in rapidly growing organisms such as yeast.

The green fluorescent protein (GFP) has become an invaluable tool for pure and applied biological research[4]. Mutagenesis of the wild-type gene yielded improved variants such as enhanced GFP (EGFP)[5,6], as well as color variants such as the cyan (CFP) and yellow (YFP) fluorescent proteins[7,8]. A recent paper[1] described a family of fluorescent proteins related to GFP. The most useful of these newly discovered proteins is DsRed, which is derived from the coral *Discosoma*. DsRed has an orange-red fluorescence with an emission maximum at 583 nm. Biophysical and X-ray crystallographic studies revealed that DsRed forms a stable tetramer, and that each monomer is structurally very similar to GFP (refs 2,9,10). The red-shifted fluorescence of DsRed relative to GFP results from a chromophore with a more extensive conjugated π-system[9,11]. DsRed fluorescence is excited optimally at 558 nm, but can also be excited by a standard 488 nm laser, allowing DsRed to be used with laser-based confocal microscopes and flow cytometers[12]. DsRed has a high quantum yield and is photostable[2]. These characteristics make DsRed an ideal candidate for fluorescence imaging, particularly for multicolor experiments involving GFP and its variants. A codon-optimized version of DsRed is now available under the name DsRed1 (ref. 13).

Despite these advantages, wild-type DsRed has several problems for use as a fluorescent reporter. When DsRed is fused to another protein, tetramerization of the DsRed domain can perturb the function and localization of the protein[14]. The DsRed tetramer also self-associates to form higher-order aggregates[3]. Perhaps the most serious problem with DsRed is that chromophore maturation is slow, with a half-time of >24 h at room temperature[2,15]. Newly synthesized DsRed develops a dim green fluorescence by forming the same chromophore that is present in GFP. A second oxidation reaction then generates the red chromophore. This slow maturation has been put to use with a DsRed variant termed the "fluorescent timer", in which the fluorescence of the initial green species is enhanced[16]. However, for most applications the slow maturation of DsRed is detrimental. In dual-label imaging with GFP, the initial green fluorescence of DsRed produces bleed-through into the GFP channel. More generally, the slow development of red fluorescence limits the intensity of the DsRed signal, particularly with rapidly growing organisms such as yeast. A variant termed DsRed2 matures faster than DsRed1, but DsRed2 still requires many hours to attain full fluorescence[13]. Here we have used random and directed mutagenesis to create improved variants of DsRed. These new variants mature rapidly, and they are more soluble than wild-type DsRed.

To identify rapidly maturing DsRed variants, we modified an earlier method for visualizing GFP fluorescence in microbial colonies[17]. Hexahistidine-tagged DsRed is produced at high levels in *Escherichia coli*. The fluorescence of the bacterial colonies is excited by placing a 520 ± 20 nm bandpass filter over the lens of a slide projector, and the emission is detected through goggles covered with a Kodak Wratten filter no. 22, which passes wavelengths >550 nm. This technique is simple and efficient.

We generated a library of mutant expression plasmids using error-prone PCR (ref. 18) to amplify the DsRed1 template. This library was transformed into *E. coli*, and over 100,000 transformant colonies were examined. Colonies producing the wild-type DsRed1 protein required two days to develop significant fluorescence, but three mutant colonies showed strong fluorescence after one day of growth. Sequencing revealed that the three mutant plasmids were distinct, but that all of them contained an N42H codon change. We therefore generated a variant that had only the N42H substitution.

The N42H variant was purified in parallel with DsRed1, and the two proteins were analyzed by spectrofluorometry. As previously observed[2], the spectra of purified DsRed1 changed over a period of days as the protein matured (data not shown). By contrast, the spectra of the purified N42H variant remained stable over time (data not shown), consistent with rapid maturation. Unfortunately, in addition to accelerating maturation, the N42H substitution altered the spectral properties of the mature protein (Fig. 1A). Mature DsRed1 is thought to be an equilibrium mixture of red fluorescent molecules and some green fluorescent molecules that are spectrally similar to GFP (refs 11,15). The GFP-like species has a blue excitation peak at ~480 nm and a green emission peak at ~500 nm; but DsRed is a tetramer, so excitation of the green molecules often results in fluorescence resonance energy transfer (FRET) with neighboring red molecules to produce red emission[2]. This FRET effect, together with the relatively low percentage of green molecules in mature DsRed1, yields a very small peak of green emission relative to the red emission (Fig. 1A). In the N42H variant, the peaks of blue excitation and green emission were dramatically enhanced (Fig. 1A), indicating that the equilibrium had shifted so that a larger percentage of the mature molecules contained the green chromophore.

Because the N42H substitution considerably increases the size of the side chain, we also tried a more conservative N42Q substitution. This mutation required two base changes and probably would not have been present in our original mutant collection. The N42Q variant retained the rapid maturation property of the N42H variant, but showed much less blue excitation and green emission (Fig. 1A). We therefore chose the N42Q variant as the starting point for further study.

Additional mutagenesis (see Supplementary Information in the Web Extras page of *Nature Biotechnology* Online) yielded DsRed variants that showed even faster maturation and lower green emission than the original N42Q variant. After six rounds of mutagenesis, we settled on three optimized variants termed DsRed.T1, DsRed.T3, and DsRed.T4 (Table 1). The spectral properties of DsRed.T4 (Fig. 1B) are

The University of Chicago, Department of Molecular Genetics and Cell Biology, 920 East 58th Street, Chicago, IL 60637.
**Corresponding author (bsglick@midway.uchicago.edu).*

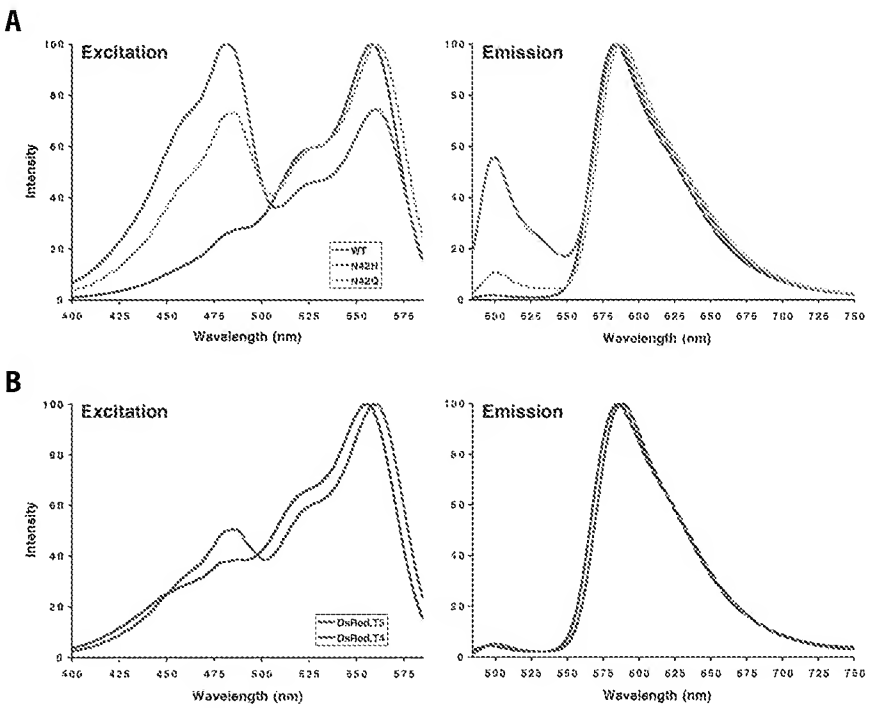

Figure 1. Normalized excitation and emission spectra of representative DsRed variants. (A) Mutating residue N42 alters the spectral properties of DsRed. Spectra are shown for DsRed1 and the N42H and N42Q variants. All three proteins were fully mature. (B) Spectra of the optimized DsRed.T3 and DsRed.T4 variants.

virtually identical to those of DsRed.T1 (data not shown) and very similar to those of the wild-type DsRed1 (Fig. 1A). Compared with DsRed.T1 and DsRed.T4, DsRed.T3 is somewhat brighter (see below) but has a significantly higher peak of blue excitation and a marginally higher peak of green emission (Fig. 1B).

The optimized DsRed variants were examined both *in vivo* and *in vitro*. As judged by colony fluorescence, colony size, and plasmid stability, these variants were less toxic to *E. coli* than DsRed1, and they developed fluorescence more efficiently at growth temperatures of 37°C and higher (data not shown). Like wild-type DsRed, the optimized variants appeared to be tetrameric: they exhibited FRET between the green and red molecules (Fig. 1B), and upon nondenaturing SDS–PAGE they migrated at the position expected for tetramers (see Supplementary Information in the Web Extras page of *Nature Biotechnology* Online). With purified DsRed1, we measured an extinction coefficient of 52,000 M^{-1} cm^{-1} and a quantum yield of ~0.7 (Table 1). A previous study of wild-type DsRed reported a similar quantum yield but a higher extinction coefficient of 75,000 M^{-1} cm^{-1} (ref. 2); the reason for this discrepancy is unclear. DsRed2 shows slight reductions in both extinction coefficient and quantum yield, resulting in a relative brightness of 0.68 compared to DsRed1 (Table 1). DsRed.T3 is nearly as bright as DsRed1. However, DsRed.T1 and DsRed.T4 are dimmer, with relative brightnesses of 0.36–0.38 compared to DsRed1.

To quantify the maturation kinetics of the DsRed variants, we performed an *in vivo* pulse-chase analysis with *E. coli* cultures growing at 37°C (Fig. 2). After a 30 min pulse of induction, protein synthesis inhibitors were added, and samples of the cultures were taken at various chase times. The average cellular fluorescence for each sample was measured by flow cytometry using a 488 nm excitation laser. Figure 2A shows the raw data, while Figure 2B shows the data normalized to a maximal fluorescence of 100%. Under these conditions DsRed1 matures with a half-time of ~11 h, although accurate measurements are difficult with DsRed1 because the fluorescence values do not reach a plateau (Fig. 2) and because some of the DsRed1 protein is degraded during the chase period (data not shown). DsRed2 matures somewhat faster, with a half-time of ~6.5 h. The rates of fluorescence acquisition for DsRed1 and DsRed2 increase after a pronounced lag phase, indicating that multiple slow steps are involved. DsRed.T3 matures with a brief lag phase and half-time of ~1.3 h. DsRed.T4 and DsRed.T1 mature with no detectable lag phase and with half-times of ~0.7 h, about 15-fold faster than DsRed1 (Fig. 2, and data not shown).

With this pulse-chase protocol, the different DsRed variants reproducibly showed distinct plateau values of average cellular fluorescence (Fig. 2A). The high signal from DsRed.T3 can be explained by the relatively strong excitation of this protein at 488 nm (see Fig. 1B). DsRed1, DsRed2, and DsRed.T4 all have similar fluorescence spectra, yet the plateau fluorescence of DsRed.T4-expressing cells is ~4-fold higher than that of DsRed1-expressing cells and ~10-fold higher than that of DsRed2-expressing cells. This result is surprising because purified DsRed.T4 is less bright than DsRed1 or DsRed2 (Table 1). We speculate that immature DsRed1 is unstable in *E. coli*, and that this problem is exacerbated with DsRed2, so that a large fraction of the newly synthesized DsRed1 and DsRed2 molecules are lost through aggregation and/or degradation. Consistent with this idea, a previous study reported that most of the newly synthesized DsRed1 molecules are degraded in *E. coli* or *Drosophila* cells[19]. Interestingly, DsRed2 gives a brighter fluorescence signal than DsRed1 in mammalian cells[13], suggesting that the efficiency of expression for a given DsRed variant may be cell type–specific.

The benefits of accelerated maturation should be particularly evident when the DsRed variants are

Table 1. Properties of the mature DsRed variants[a]

DsRed variant	Excitation maximum (nm)	Emission maximum (nm)	Maximal extinction coefficient (M^{-1} cm^{-1})	Quantum yield	Relative brightness[b]	Maturation half-time (h)[c]
DsRed1	558	583	52,000	0.68	(1.00)	11
DsRed2	561	587	43,800	0.55	0.68	6.5
DsRed.T1	554	586	30,100	0.42	0.36	0.70
DsRed.T3	560	587	49,500	0.59	0.83	1.3
DsRed.T4	555	586	30,300	0.44	0.38	0.71

[a]DsRed1 is identical to wild-type DsRed except for a valine insertion after the start codon. DsRed2 lacks this extra valine. Relative to wild-type DsRed, the other variants contain the following substitutions, where P(–4)L indicates a codon change in the polylinker upstream of the start codon.
DsRed2: R2A, K5E, K9T, V105A, I161T, S197A.
DsRed.T1: P(–4)L, R2A, K5E, N6D, T21S, H41T, N42Q, V44A, C117S, T217A.
DsRed.T3: P(–4)L, R2A, K5E, N6D, T21S, H41T, N42Q, V44A, A145P.
DsRed.T4: P(–4)L, R2A, K5E, N6D, T21S, H41T, N42Q, V44A, A145P, T217A.
[b]Brightness is determined by the product of the extinction coefficient and the quantum yield. Relative brightness is calculated by defining the brightness of DsRed1 as 1.00.
[c]The half-times for maturation were estimated graphically using the experimental protocol of Figure 2. Values listed are the averages from two separate experiments; for each DsRed variant, the numbers obtained in the two experiments were within 15% of one another.

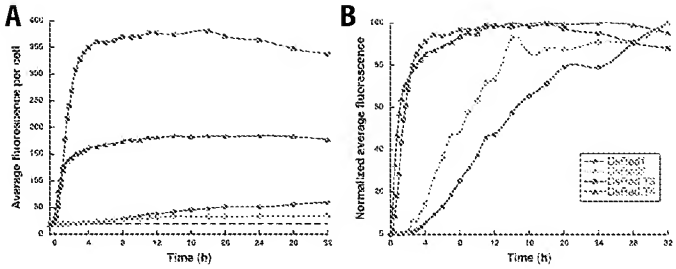

Figure 2. Maturation kinetics of DsRed variants. Logarithmically growing *E. coli* cultures were treated with the inducer isopropyl β-D-thiogalactopyranoside (IPTG) for 30 min to generate a pulse of expression for each variant. A chase was then initiated (at time 0 on the graphs) by adding protein synthesis inhibitors and continuing the 37°C incubation. Aliquots of the cultures were removed at the indicated times and subsequently analyzed by flow cytometry to determine the average intensity of red fluorescence per cell. The background fluorescence (dashed line) was measured using cells carrying the empty pQE81 plasmid. Plotted on the two graphs are (A) the raw fluorescence values, or (B) the values obtained by subtracting the fluorescence present at time 0 and normalizing to a maximum signal of 100% for each DsRed variant. A slight decline at later time points in the average fluorescence values for DsRed.T3 and DsRed.T4 probably reflects cell lysis. In a control culture, protein synthesis inhibitors were added simultaneously with IPTG to cells carrying the DsRed.T3 expression plasmid; as expected, those cells remained nonfluorescent (data not shown). Immunoblotting indicated that during the chase period, the amount of DsRed2, DsRed.T3, and DsRed.T4 protein in the cultures remained essentially constant, whereas the amount of DsRed1 protein progressively declined to about half of its initial level (data not shown).

produced in a rapidly growing organism. To test this prediction, we targeted different DsRed variants to yeast mitochondria. The parental yeast strain also contained an EGFP-tagged marker for Golgi cisternae[20]. With mitochondrially targeted DsRed1, the fluorescence was extremely faint in cells from growing cultures, and only became readily visible in a subset of the cells once the cultures reached stationary phase (data not shown). By contrast, mitochondrially targeted DsRed.T4 consistently gave a strong fluorescence signal in cells from growing cultures (Fig. 3). As shown in the merged image, we observed no detectable bleed-through of DsRed.T4 fluorescence into the green channel or of EGFP fluorescence into the red channel. Similar results were obtained with mitochondrially targeted DsRed.T3 (data not shown). However, with other fusion constructs we found that when a large amount of DsRed.T3 was concentrated in a small region of the cell, some bleed-through occurred into the green channel (not shown). Therefore, DsRed.T4 is the protein of choice for obtaining a clean separation of red and green fluorescence signals.

These results confirm that random mutagenesis followed by screening is a powerful method for creating improved fluorescent proteins[5,6]. Our key finding is that Asn42 substitutions such as N42Q dramatically accelerate chromophore formation. It is known that the side chain of Asn42 faces the interior of the protein and helps to position the Gln66 side chain, which becomes part of the chromophore[10], but further work will be needed to clarify how Asn42 substitutions accelerate DsRed maturation.

A side effect of Asn42 substitutions is a pronounced increase in blue excitation and green emission (Fig. 1A). Mature wild-type DsRed appears to be an equilibrium mixture of a red species and a green species[11,15], and the Asn42 substitutions evidently shift the equilibrium to yield a higher percentage of the green species. The nature of this equilibrium is unknown. Perhaps the final oxidation step that generates the red chromophore[11] is readily reversible. An alternative possibility is that internal water molecules present in the native protein[10] reversibly hydrate the acylamine substituent in the chromophore to generate a green species[11]. Regardless of the mechanism, it is clear that many residues in DsRed can influence the equilibrium between the red and green species[15]. By introducing a series of additional substitutions into the N42Q background, we could suppress nearly all of the blue excitation and green emission that were conferred by N42Q while preserving the rapid maturation (Fig. 1 and Table 1).

Another improvement over wild-type DsRed was achieved by decreasing the net charge near the N terminus. The resulting DsRed variants show reduced aggregation *in vitro* (see Supplementary Information in the Web Extras page of *Nature Biotechnology* Online) and *in vivo*[13]. We discovered this effect by random mutagenesis, but a similar set of substitutions was engineered into DsRed2 by researchers seeking to diminish the overall charge of the protein (S. Lukyanov, pers. commun.). Wild-type DsRed is unusually basic, with a predicted pI of 8.0, and probably associates nonspecifically with anionic cellular components. In addition, basic patches on the surface of a DsRed tetramer may interact with acidic patches on a second tetramer to cause higher-order aggregation. This interaction of DsRed with other macromolecules is evidently reduced by eliminating the cluster of positive charges near the N terminus.

The end result of our work is a pair of optimized variants termed DsRed.T3 and DsRed.T4. DsRed.T3 matures rapidly, and the purified protein is nearly as bright as mature wild-type DsRed (Table 1), making this variant well suited to single-color imaging of red fluorescence. DsRed.T3 has a higher peak of blue excitation and a slightly higher peak of green emission than wild-type DsRed (Fig. 1B), resulting in some contamination of the GFP signal in dual-color experiments. However, this contamination is usually minor. The enhanced blue excitation of DsRed.T3 can actually be advantageous, for example, if the fluorescence is being excited by a 488 nm laser (Fig. 2). DsRed.T4 has fluorescence spectra very similar to those of wild-type DsRed (Fig. 1B) and yields negligible contamination of the GFP signal (Fig. 3). Although purified DsRed.T4 is only about half as bright as DsRed.T3, this effect is partially offset *in vivo* because DsRed.T4 matures nearly twice as fast as DsRed.T3

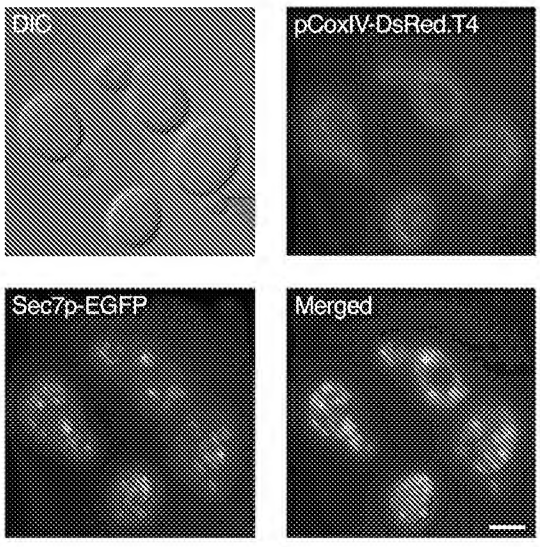

Figure 3. Simultaneous visualization of DsRed.T4 and EGFP in yeast. DsRed.T4 was targeted to the mitochondrial matrix of *Saccharomyces cerevisiae* by fusion to the presequence of Cox4p. The pCox4-DsRed.T4 fusion protein was produced in a strain that also contained Sec7p-EGFP, a marker for Golgi cisternae[20]. Cells from a logarithmically growing culture were imaged using either a Texas Red filter set (red) or an EGFP filter set (green). In addition, the cells were visualized by differential interference contrast (DIC) microscopy. As shown in the merged image, the DsRed.T4 and EGFP signals are easily resolved. Scale bar, 2 μm.

(Table 1). Thus, DsRed.T4 is probably the best variant for most applications. DsRed.T1 is essentially identical to DsRed.T4 (Table 1), except that DsRed.T1 lacks cysteine residues and therefore might fold more efficiently in the oxidizing environment of the secretory pathway.

DsRed.T4 is a suitable template for further mutagenesis to produce additional variants. An obvious goal is to identify mutations that preserve the advantages of DsRed.T4 while restoring a wild-type level of brightness. Perhaps the biggest remaining challenge is to eliminate the tetramerization of DsRed. Although tetramerization is not a hindrance if unmodified DsRed is used to label entire cells or organelles, fusions of DsRed to oligomeric or membrane-associated proteins often lead to massive aggregation[14]. Creating a monomeric DsRed variant should be feasible because DsRed is structurally very similar to GFP, which is a monomer with only a weak tendency to dimerize[4].

The generation of new DsRed variants is likely to involve both random and directed mutagenesis. For directed mutagenesis studies, it is worth noting that five of the substitutions present in DsRed.T4 (R2A, H41T, N42Q, A145P, and T217A) replace a given residue with a residue that is more generally conserved in the family of DsRed homologs[1,9]. Thus, sequence comparisons between DsRed and its relatives can suggest mutations that are likely to produce useful variants.

Experimental protocol

Mutagenesis and screening. For mutagenesis, a wild-type or mutant DsRed gene present in the pDsRed1-N1 vector (Clontech, Palo Alto, CA) was excised with *Nhe*I and *Hpa*I and used as a template for error-prone PCR (ref. 18). The amplified product was digested with *Bam*HI and *Bsa*BI, gel purified, and ligated between the *Bam*HI and *Ecl*136II sites of the pQE31 expression vector (Qiagen, Valencia, CA), which encodes an N-terminal hexahistidine tag. The library of mutated DsRed genes was transformed into *E. coli* strain DH10B.

For rounds 1–3 of the mutagenesis, 50,000–100,000 colonies were screened for bright fluorescence using the slide projector assay described in the text. For round 4, ~4,000 brightly fluorescent colonies were picked into wells of 96-well plates, then grown to saturation, lysed with B-PER II reagent (Pierce, Rockford, IL), and centrifuged for 5 min at 2,500 *g*. The supernatants were transferred to a second set of 96-well plates, and the fluorescence signals from the pellets and supernatants were compared visually using the slide projector assay. Clones that showed an elevated ratio of soluble to insoluble fluorescence were analyzed further. For round 5, 10 pools of ~10,000 mutant clones each were recovered from the transformation plates and subjected to cell sorting using a Becton Dickinson FACStarPlus flow cytometer. Fluorescence signals were measured simultaneously in the green (FL-1) and red (FL-2) channels, and cells were collected if they showed strong red fluorescence but reduced green fluorescence.

Purification and spectral analysis of the DsRed variants. To purify the hexahistidine-tagged proteins, a fluorescent protein gene in the pQE31 vector was transformed into *E. coli* cells carrying the pREP4 repressor plasmid (Qiagen). A 250 ml culture was grown to an OD_{600} of 0.5 and then induced with 1 mM isopropyl-β-D-thiogalactoside (IPTG) for 6–8 h at 37°C. The cells were lysed with 10 ml of B-PER II and centrifuged for 20 min at 27,000 *g*. Detergent was removed from the supernatant by adding NaCl to 300 mM and centrifuging for 10 min at 2,500 *g*. After adding 1 ml of Ni^{2+}-NTA-agarose beads (Qiagen), the tube was mixed end-over-end for 1 h. The beads were washed three times with 10 ml of 300 mM NaCl, 20 mM imidazole-HCl, pH 7.4, 0.5% Triton X-100, and then three times with the same buffer lacking Triton X-100. The fluorescent protein was eluted with 2.5 ml of 300 mM imidazole-HCl, pH 7.4, and dialyzed into 50 mM Na^+-HEPES, pH 7.5, 100 mM NaCl, 1 mM EDTA.

Corrected excitation and emission spectra of purified DsRed variants, diluted to an A_{558} of <0.04 in Na^+-HEPES, pH 7.5, 100 mM NaCl, 1 mM EDTA, were acquired with a Horiba FluoroMax-3 spectrofluorometer. The scanning windows were 1 nM. Emission was measured at 600 nm for the excitation spectra, and excitation was at 470 nm for the emission spectra. To determine extinction coefficients, the fluorescent protein concentrations were assayed using the BCA method (Pierce), and the absorbances of the proteins at their excitation maxima were measured using a Spectronic Unicam GENESYS 10 UV spectrophotometer. Quantum yields were determined as described[2,21] using ethanolic rhodamine 101 as a reference; for these measurements the excitation wavelength was 535 nm and the fluorescence emission was integrated from 550-800 nm.

Measurement of maturation kinetics. Genes encoding the DsRed variants were cloned into the pQE81 expression vector (Qiagen) and transformed into *E. coli*. Bacterial cultures growing with aeration at 37°C were induced with 1 mM IPTG for 30 min to generate a pulse of expression for each DsRed variant. A chase was then initiated by inhibiting protein synthesis with a mixture of 170 μg/ml chloramphenicol, 30 μg/ml kanamycin, and 50 μg/ml tetracycline. At the designated time points, aliquots of the cultures were removed, adjusted to 15% glycerol, and frozen at –80°C. These aliquots were later thawed rapidly and evaluated using a Becton Dickinson FACScan flow cytometer to determine the average intensity of red fluorescence (channel FL-2) per cell. A portion of each aliquot was precipitated with trichloroacetic acid, then subjected to SDS–PAGE and immunoblotting with an anti-hexahistidine monoclonal antibody (Qiagen) to measure the total amount of DsRed polypeptide in the cultures.

Fluorescence microscopy of yeast. A *CEN* plasmid derived from pRS315 (ref. 22) and carrying a pCox4-DsRed1 fusion gene under the control of the *ADH1* promoter was used. Derivatives of this plasmid were created by replacing the DsRed1 coding sequence with the coding sequence of DsRed.T3 or DsRed.T4. These plasmids were introduced into *S. cerevisiae* strain BGY101, which carries a chromosomal *SEC7-EGFPx3* gene[20]. Cells from the resulting yeast strains were grown in minimal glucose medium and fixed, and projected fluorescence images were acquired as described[23].

Note: Supplementary information can be found on the Nature Biotechnology *website in Web Extras (http://biotech.nature.com/web_extras).*

Acknowledgments

Thanks to Sergey Lukyanov for sharing unpublished data, to Hiromi Sesaki and Rob Jensen for providing the pCox4-DsRed expression plasmid, to Susan Lindquist for use of the spectrofluorometer, to Dan Strongin for assistance with Supplementary Figure 1A, and to members of the Glick lab for feedback on the manuscript. This work was supported by grants from the National Science Foundation (MCB-9875939) and the American Cancer Society (RPG-00-245-01-CSM).

Received 21 August 2001; accepted 21 November 2001

1. Matz, M.V. *et al.* Fluorescent proteins from nonbioluminescent Anthozoa species. *Nat. Biotechnol.* **17**, 969–973 (1999).
2. Baird, G.S., Zacharias, D.A. & Tsien, R.Y. Biochemistry, mutagenesis, and oligomerization of DsRed, a red fluorescent protein from coral. *Proc. Natl. Acad. Sci. USA* **97**, 11984–11989 (2000).
3. Jakobs, S., Subramaniam, V., Schönle, A., Jovin, T.M. & Hell, S.W. EGFP and DsRed expressing cultures of *Escherichia coli* imaged by confocal, two-photon and fluorescence lifetime microscopy. *FEBS Lett.* **479**, 131–135 (2000).
4. Sullivan, K.F. & Kay, S.A. (eds) *Green fluorescent proteins.* Vol. 58, *Methods in Cell Biology.* (Academic Press, San Diego, CA; 1999).
5. Heim, R., Cubitt, A.B. & Tsien, R.Y. Improved green fluorescence. *Nature* **373**, 663–664 (1995).
6. Cormack, B.P., Valdivia, R.H. & Falkow, S. FACS-optimized mutants of the green fluorescent protein (GFP). *Gene* **173**, 33–38 (1996).
7. Heim, R. & Tsien, R.Y. Engineering green fluorescent protein for improved brightness, longer wavelengths and fluorescent resonance energy transfer. *Curr. Biol.* **6**, 178–182 (1996).
8. Miyawaki, A. *et al.* Fluorescent indicators for Ca^{2+} based on green fluorescent proteins and calmodulin. *Nature* **388**, 882–887 (1997).
9. Wall, M.A., Socolich, M. & Ranganathan, R. The structural basis for red fluorescence in the tetrameric GFP homolog DsRed. *Nat. Struct. Biol.* **7**, 1133–1138 (2000).
10. Yarbrough, D., Wachter, R.M., Kallio, K., Matz, M.V. & Remington, S.J. Refined crystal structure of DsRed, a red fluorescent protein from coral, at 2.0-Å resolution. *Proc. Natl. Acad. Sci. USA* **98**, 462–467 (2001).
11. Gross, L.A., Baird, G.S., Hoffman, R.C., Baldridge, K.K. & Tsien, R.Y. The structure of the chromophore within DsRed, a red fluorescent protein from coral. *Proc. Natl. Acad. Sci. USA* **97**, 11990–11995 (2000).
12. Hawley, T.S., Telford, W.G., Ramezani, A. & Hawley, R.G. Four-color flow cytometric detection of retrovirally expressed red, yellow, green, and cyan fluorescent proteins. *BioTechniques* **30**, 1028–1034 (2001).
13. Living Colors™ DsRed2. *CLONTECHniques* **XVI**, 2–3 (2001).
14. Lauf, U., Lopez, P. & Falk, M.M. Expression of fluorescently tagged connexins: a novel approach to rescue function of oligomeric DsRed-tagged proteins. *FEBS Lett.* **498**, 11–15 (2001).

15. Wiehler, J., von Hummel, J. & Steipe, B. Mutants of *Discosoma* red fluorescent protein with a GFP-like chromophore. *FEBS Lett.* **487**, 384–389 (2001).
16. Terskikh, A. *et al.* "Fluorescent timer": protein that changes color with time. *Science* **290**, 1585–1588 (2000).
17. Cronin, S. & Hampton, R. A genetics-friendly GFP assay. *Trends Cell Biol.* **9**, 36 (1999).
18. Cadwell, R.C. & Joyce, G.F. Mutagenic PCR. In *PCR Primer. A laboratory manual.* (eds Dieffenbach, C.W. & Dveksler, G.S.) 583–589 (Cold Spring Harbor Laboratory Press, Cold Spring Harbor, NY; 1995).
19. Verkhusha, V.V. *et al.* An enhanced mutant of red fluorescent protein DsRed for double labeling and developmental timer of neural fiber bundle formation. *J. Biol. Chem.* **276**, 29621–29624 (2001).
20. Rossanese, O.W. *et al.* A role for actin, Cdc1p and Myo2p in the inheritance of late Golgi elements in *Saccharomyces cerevisiae*. *J. Cell Biol.* **153**, 47–61 (2001).
21. Lakowicz, J.R. *Principles of fluorescence spectroscopy*, Edn. 2. (Kluwer Academic/Plenum Publishers, New York, NY; 1999).
22. Sikorski, R.S. & Hieter, P. A system of shuttle vectors and yeast host strains designed for efficient manipulation of DNA in *Saccharomyces cerevisiae*. *Genetics* **122**, 19–27 (1989).
23. Rossanese, O.W. *et al.* Golgi structure correlates with transitional endoplasmic reticulum organization in *Pichia pastoris* and *Saccharomyces cerevisiae*. *J. Cell Biol.* **145**, 69–81 (1999).

A variant of yellow fluorescent protein with fast and efficient maturation for cell-biological applications

Takeharu Nagai[1], Keiji Ibata[2], Eun Sun Park[1], Mie Kubota[3], Katsuhiko Mikoshiba[2] and Atsushi Miyawaki[1]*

The green fluorescent protein (GFP) from the jellyfish *Aequorea victoria* has provided a myriad of applications for biological systems[1]. Over the last several years, mutagenesis studies have improved folding properties of GFP (refs 1,2). However, slow maturation is still a big obstacle to the use of GFP variants for visualization. These problems are exacerbated when GFP variants are expressed at 37°C and/or targeted to certain organelles. Thus, obtaining GFP variants that mature more efficiently is crucial for the development of expanded research applications. Among *Aequorea* GFP variants, yellow fluorescent proteins (YFPs) are relatively acid-sensitive, and uniquely quenched by chloride ion (Cl^-)[3]. For YFP to be fully and stably fluorescent, mutations that decrease the sensitivity to both pH and Cl^- are desired. Here we describe the development of an improved version of YFP named "Venus". Venus contains a novel mutation, F46L, which at 37°C greatly accelerates oxidation of the chromophore, the rate-limiting step of maturation. As a result of other mutations, F64L/M153T/V163A/S175G, Venus folds well and is relatively tolerant of exposure to acidosis and Cl^-. We succeeded in efficiently targeting a neuropeptide Y-Venus fusion protein to the dense-core granules of PC12 cells. Its secretion was readily monitored by measuring release of fluorescence into the medium. The use of Venus as an acceptor allowed early detection of reliable signals of fluorescence resonance energy transfer (FRET) for Ca^{2+} measurements in brain slices. With the improved speed and efficiency of maturation and the increased resistance to environment, Venus will enable fluorescent labelings that were not possible before.

[1]*Laboratory for Cell Function and Dynamics, Advanced Technology Development Center,* [2]*Laboratory for Developmental Neurobiology, and* [3]*Laboratory for Molecular Dynamics of Mental Disorder, Brain Science Institute, RIKEN, 2-1 Hirosawa, Wako-city, Saitama, 351-0198, Japan.* **Corresponding author (matsushi@brain.riken.go.jp).*

By randomly mutagenizing pericams (circularly permuted GFPs that sense Ca^{2+})[4], we found several mutations that improved their maturation. Of particular interest was the mutation F46L, which greatly improved the maturation at 37°C. Considering that YFP was the source of pericams, we were curious if F46L could increase the maturation efficiency of YFP. The effect of F46L was studied in EYFP (S65G/S72A/T203Y), a widely used YFP variant. The effect of the well-known folding mutations, F64L/M153T/V163A/S175G, on EYFP was also examined. There have been no reports on the introduction of those mutations to YFP, although these mutations have been purported to increase folding efficiency in other GFP variants. By employing our new protocol for multiple-site mutagenesis[5], we were able to introduce the four common folding mutations simultaneously into EYFP to create SEYFP (super-EYFP) (EYFP-F64L/M153T/V163A/S175G). EYFP-F46L and SEYFP-F46L were obtained by introducing F46L into EYFP and SEYFP, respectively. We cultured the *Escherichia coli* clones producing the four YFPs at 37°C, and compared fluorescence intensities of the cell suspensions. F46L greatly facilitated the maturation of YFP (Fig. 1A, Table 1). The purified YFP variants exhibited exactly the same excitation and emission spectra, and almost equivalent extinction coefficients and fluorescence quantum yields, ranging from 78,700 to 101,000 $M^{-1}cm^{-1}$ and from 0.56 to 0.61, respectively (Table 1).

Newly synthesized GFP polypeptides need to mature properly before emitting fluorescence. The maturation process involves two steps: folding and chromophore formation. First, the protein folds into a native conformation, and then, an internal tripeptide cyclizes and is oxidized. The folding efficiency of the YFP variants was assessed at 37°C by monitoring the acquisition of fluorescence upon re-naturation of urea-denatured protein with a mature chromophore[6]. As the protein refolds, the matured chromophore is buried inside the β-barrel, resulting in recovery of fluorescence (Fig. 1B). The re-naturation of all the YFP variants proceeded through two distinct kinetic phases as earlier reported[6]. The first-order rate constants for the initial phase varied among the YFP variants (Table 1). Both SEYFP and SEYFP-F46L, containing the mutations F64L/M153T/V163A/S175G, recovered rapidly, with rate constants (K_{fold} values) of 0.066 s^{-1} and 0.0562 s^{-1}, respectively. The effect of F46L was less potent than that of the mutations F64L/ M153T/V163A/S175G. Therefore, the common folding mutations were effective in facilitating folding of YFP at 37°C.

Next, the chromophores of the urea-denatured YFPs were reduced with 5 mM dithionite[6]. At 37°C, re-naturation and re-oxidation were initiated by dilution. Because oxidation is the slowest step, the observed overall rate of fluorescence recovery should represent the rate of oxidation of the cyclized chromophore. The rate constants for their initial phases (K_{ox} values) were compared (Fig. 1C). While SEYFP and SEYFP-F46L gave similar K_{fold} values, the speed and yield of the re-naturation from denatured/reduced protein was significantly improved by F46L (Fig. 1D; K_{ox} values in Table 1, 0.00236 s^{-1} vs. 0.00804 s^{-1}). EYFP-F46L also showed faster re-oxidation than SEYFP.

The above results indicate that F46L accelerates the oxidation step, leading to the enhancement of fluorescence development of YFP at 37°C. The SEYFP-F46L variant folds and forms the chromophore very efficiently at 37°C, giving off a bright yellowish light. Venus is the brightest object in our nighttime sky except for the moon, and thus we call the SEYFP-F46L variant "Venus". To examine whether F46L favors any other *Aequorea* GFP variants, we introduced F46L